Switchable self-defocusing and focusing in nearly isotropic photonic crystals via enhanced inverse diffraction

Zhixiang Tang,[1,2,3] Lei Zhao,[4] Zhan Sui,[4] Yanhong Zou,[2,5] Shuangchun Wen,[2,5,*] Aaron Danner,[3] and Chengwei Qiu[3]

[1]*College of Computer Science and Electronic Engineering, Hunan University, Changsha 41008, China*

[2]*Key Laboratory for Micro-/Nano- Optoelectronic Devices of Ministry of Education, Hunan University, Changsha 41008, China*

[3]*Department of Electrical and Computer Engineering, National University of Singapore, 4 Engineering Drive 3, Singapore 117576*

[4]*Research Center of Laser Fusion, Chinese Academic of Engineering Physics, Mianyang 621900, China*

[5]*College of Physics and Microelectronic Science, Hunan University, Changsha 41008, China*

(Received 5 March 2015; published 18 June 2015)

Generally, optical diffraction is only weakly dependent on the refractive index of a medium in which light propagates. In this paper, diffraction in a nearly isotropic Kerr photonic crystal (PhC) made of silicon pillars embedded in nonlinear carbon disulfide ambient was reversed and enhanced by its linear refractive index, which is negative and much less than unity. The effective nonlinear refractive index coefficient n_2 of the PhC was found by fitting spectral broadening induced by self-phase modulation. The enhanced inverse diffraction, attributed to positive n_2, allows self-defocusing in one single PhC. More interestingly, the same PhC can selectively exhibit dual functionalities, i.e., self-defocusing and self-focusing, based on the wavefront property of a given input beam. Our results may pave the way for protecting nanostructured photonic devices from laser damage and provide a method for controlling wavefronts.

DOI: 10.1103/PhysRevA.91.063824 PACS number(s): 42.70.Qs, 42.65.Jx

I. INTRODUCTION

When light propagates in a homogeneous medium, optical diffraction, a geometrical effect leading to a broadening of the spatial intensity profile, usually depends only on the medium's refractive index. For linear propagation of a Gaussian beam of waist w_0, its spatial intensity profile in the far field spreads with an angle of $\theta = \lambda_0/(\pi n_0 w_0)$, where λ_0 and n_0 are the wavelength in vacuum and the linear refractive index of a medium in which light propagates, respectively [1]. On the other hand, in nonlinear propagation of a high-power laser beam, diffraction is usually overwhelmed by self-focusing induced by the intensity-dependent refractive index, which often results in laser damage due to greatly increased peak power in optical devices [2,3]. In order to protect optical devices in the presence of high-power laser systems, self-defocusing, which is another type of spatial manifestation of the intensity-dependent refractive index, is advantageous, because it can lead to spatial broadening of a beam.

The intensity-dependent refractive index is usually given by $n(|E|^2) = n_0 + n_2|E|^2$, where n_0 and n_2 are the linear refractive index and the nonlinear refractive index coefficient of the Kerr medium, respectively. Therefore, self-defocusing in this medium requires n_0 and n_2 be of opposite sign [4–8]. Unfortunately, most natural materials have simultaneously a positive n_0 and n_2. Based on inverse diffraction originating from the guided modes coupling, Morandotti *et al.* have experimentally demonstrated controllable self-focusing and self-defocusing in planar waveguide arrays [9,10], but these interesting phenomena are primarily confined within a very thin surface region. We use a different approach and are able to demonstrate self-defocusing in a nearly isotropic photonic crystal (PhC) bulk material, with positive effective n_2, via enhanced inverse diffraction; this is impossible in natural media.

PhCs are manmade periodic structures that can exhibit unusual linear optical properties not attainable in natural materials such as negative refractive index [11–15] and an artificial magnetic response [16,17]. Recently, many researchers have studied the influences of infiltrating nonlinear elements into these periodic nanostructures [18–26]. Although numerous results about nonlinear PhCs have been reported, only a few papers have considered the potential of controlling of self-focusing in nonlinear PhCs [20,21]. Moreover, their controlling mechanisms, which are similar to those of focusing microwave radar signals by virtual hyperbolic metamaterials [27], were based on the strong and sensitive anisotropy in the self-collimation frequency range whose bandwidth is very narrow. Therefore, self-defocusing in an isotropic nanostructure made of common Kerr materials has still not been reported, which is the subject of the present work. Interestingly, our proposed PhC design allows switchable dual functionalities in the same nanostructure, i.e., self-defocusing or self-focusing, depending on whether the incident beam has a divergent or convergent wavefront.

II. EFFECTIVE PARAMETERS OF A NONLINEAR PhC

A. The method for retrieving n_2 of a nonlinear PhC

In general, whether self-focusing or self-defocusing occurs in a homogeneous Kerr medium (HKM) is determined by n_0 and n_2. For PhCs, n_0 can be easily derived from the photonic band structure. The nonlinear refractive index coefficient n_2, which plays the crucial role in self-defocusing, cannot be so easily retrieved and a programmatic approach of determining it for any given structure is needed. It is noted that Smith *et al.* have proposed a few retrieval methods for effective susceptibility of nonlinear metamaterials when unit cells are much smaller than the operating wavelength [23–26]. However, their methods assumed a nondepleted pump approximation, which is not valid in the presence of the optical Kerr effect. In this regard,

*scwen@hnu.edu.cn

the method to be presented here, which is based on fitting spectral broadening induced by self-phase modulation (SPM), can unambiguously retrieve the effective n_2 of an isotropic nonlinear PhC, enabling a fundamentally indispensable way of rigorously studying Kerr nonlinear effects in PhCs.

For nonlinear propagation of a chirped Gaussian pulse [28–31], if the propagation distance is much less than the pulse's dispersion length and losses of the HKM are low enough, the broadened spectrum induced by SPM can be given by [22]

$$S(L,f)=\left|\int_{-\infty}^{+\infty}E_0e^{-T^2/2T_0^2}\exp\left[i\left(n_2E_0^2e^{-T^2/T_0^2}\frac{2\pi f_0}{c}L-C_p\frac{T^2}{2T_0^2}\right)+i2\pi(f-f_0)T\right]dT\right|^2, \quad (1)$$

where E_0, f_0, C_p, and T_0 are the peak amplitude, central frequency, chirp parameter, and temporal half-width (at the $1/e$-intensity point) of the input pulse, respectively. c denotes the speed of light in a vacuum. n_2 and L, the nonlinear refractive index coefficient and the length, are the only two parameters of the HKM. Thus, the SPM-induced spectral broadening for a given chirped Gaussian pulse propagating through an unknown nanostructure made of a Kerr medium is actually only represented by the unknown n_2 because the length L can be measured directly.

B. The linear refractive index (n_0) of the PhC

Taking a two-dimensional PhC as an example, the PhC consists of a square-lattice of silicon cylinders immersed in liquid carbon disulfide (CS_2) background. At the operating wavelength $\lambda_0 = 10.6\,\mu$m (the central wavelength of carbon dioxide laser, $f_0 = c/\lambda_0 = 28.283$ THz), the intensity-dependent refractive index of CS_2 is $n(|E|^2) = 1.63 + 1.67 \times 10^{-20}\ \mathrm{m^2/V^2}|E|^2$ [32], and the dielectric constant of silicon is $\varepsilon = 12.96$. The silicon cylinder has a radius of $r = 0.22a$, where a is the lattice constant. For this PhC, we only considered the TM polarization; i.e., the electric field E_z is parallel to these cylinders.

The photonic band structure was calculated by using the plane wave expansion method and is plotted in Fig. 1(b), in which the frequency is normalized as a/λ. From the photonic band structure, it can be seen that the second band (green line marked with circles) has a distinct downward curvature near the Brillouin zone center Γ, suggesting that the refractive indexes of the PhC in this frequency region are negative ($n_0 < 0$) and diffraction in the PhC is reversed [9,10]. To clearly display this interesting phenomenon, we took a normalized frequency at 0.4 [the dashed line in Fig. 1(b)] as the operating frequency, at which the effective refractive index was about $n_0 = -0.23$. With a n_0 that is much less than unity, wavefront in the PhC is enlarged and distinguishable. Moreover, the expansion rate induced by diffraction was amplified remarkably [1]. Different from controlling nonlinear effect by strong anisotropy originated from flat equifrequency contour [20,21], the equifrequency contour of our PhC at the operating frequency was nearly a circle as shown in the inset of Fig. 1(b), indicating relatively good isotropy of the PhC. It is noted that two degenerate modes from the second and the third band coexist at the normalized frequency of 0.4. However, only the mode from the second (around Γ) band is considered because the mode from the third band (around M) will not be excited for the propagation of Gaussian beams with narrow spatial spectral [33].

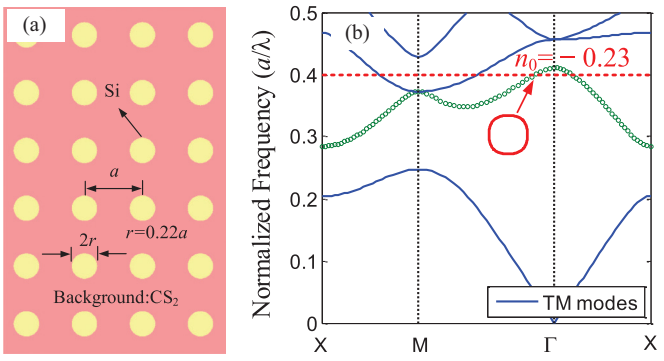

FIG. 1. (Color online) (a) A sketch of the two-dimensional PhC and (b) the photonic band structure of the PhC studied in this letter. At the operating freqency $n_f = 0.4$, the equifrequency contour of the PhC is shown in the inset to indicate its relatively good isotropy.

C. Retrieving n_2 of the nonlinear PhC

The method proposed in Sec. I is employed to retrieve the PhC's effective n_2. Figure 2 shows the retrieving sketch and procedure. First, we employed the nonlinear finite-difference time-domain (FDTD) method [34] to obtain the broadened spectra by simulating chirped Gaussian pulses propagating through the PhC. Then, via changing the n_2, several spectra of the same pulse propagating in a HKM of the same length as the PhC structure were calculated theoretically through Eq. (1). Finally, we retrieved the effective n_2 of the nonlinear PhC by matching the theoretically calculated spectrum with the one obtained from the FDTD simulation.

In this paper, we simulated two chirped Gaussian pulses propagating along the ΓX direction in the nonlinear PhC. The central frequency, temporal half-width, and chirp parameters of the input Gaussian pulses were taken as $f_0 = 28.283$ THz, $T_0 = 22.10$ ps, and $C_p = \pm 1$, respectively. The input pulses with peak amplitude $E_0 = 2.0 \times 10^8$ V/m were detected after passing through a $701a$-thick (about $L = 3000\,\mu$m) nonlinear PhC. Note that all the parameters were carefully chosen to ensure that the group-velocity dispersion effect was negligible compared to the SPM [35]. Performing Fourier transformation on the detected pulses, we finally obtained the normalized spectra illustrated in Fig. 3. Evidently, the spectrum detected from the positively chirped pulse was broader than that from the pulse with negative chirp, suggesting a positive n_2 of the PhC. Moreover, the peak at high frequency is slightly lower than that at low frequency. These asymmetrical spectra are attributed to the decreasing transmittance at the higher

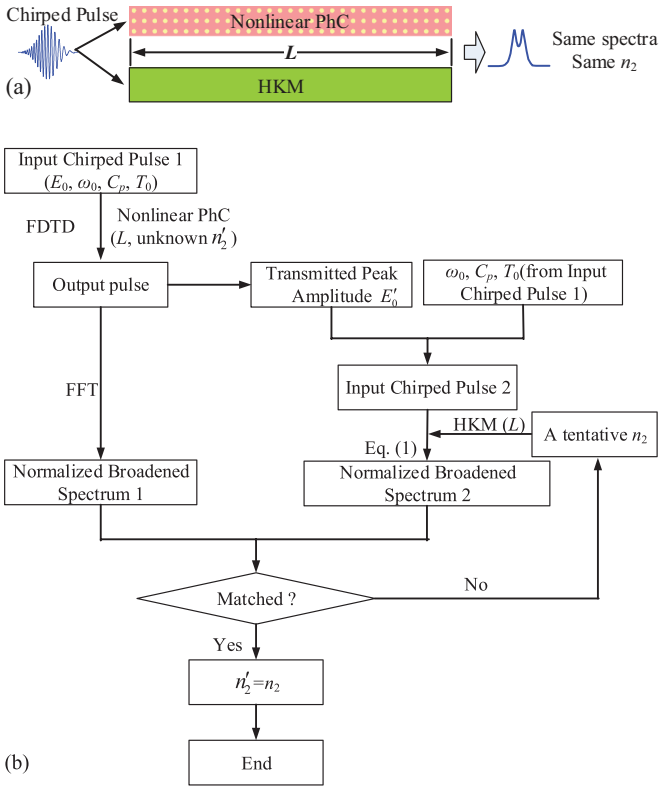

FIG. 2. (Color online) (a) Sketch and (b) procedure for retrieving n_2 of a nonlinear PhC based on SPM-induced spectral broadening.

frequency, which is closer to the second bandgap as shown in the photonic band structure in Fig. 1(b).

Capturing the peak amplitude from the detected data and substituting it together with the other parameters of the input pulse into Eq. (1), we theoretically obtained serveral broadened spectra for the same pulse propagating in a HKM of the same length as the nonlinear PhC while iterating n_2. When $n_2 = 6.2 \times 10^{-20}\,\mathrm{m^2/V^2}$, the theoretical spectra is in good agreement with those obtained from FDTD simulations as plotted in Fig. 3. It shows that the spectrum of $C_p = -1$ fits better than that of $C_p = +1$. It is worth pointing out

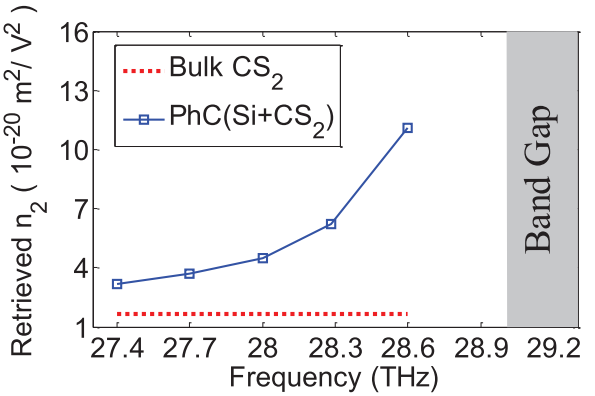

FIG. 4. (Color online) Retrieved n_2 of the nonlinear PhC in the second band.

that the retrieved n_2 of our PhC at a fixed frequency are almost invariable with the pulse's parameters as long as the group-velocity dispersion and losses can be neglected in the simulations [36]. Moreover, we also retrieved the effective n_2 at the other four frequencies in the second band and plotted these in Fig. 4. Obviously, n_2 increases rapidly with frequency. The enhancement of nonlinearity in this Kerr PhC is mainly resulted from the field localization in the nonlinear background and small group velocity of the high frequency in the upper part of the second band [37–39]. Significantly, n_2 of the nonlinear PhC at high frequencies are even much greater than that of Kerr medium CS_2, the only nonlinear component of the PhC. It indicates that the nonlinearity of the nonlinear medium can be greatly enhanced by the insertion of linear periodic components inside.

III. SELF-DEFOCUSING VIA ENHANCED INVERSE DIFFRACTION

To demonstrate nonlinear beam propagation in this PhC, we applied a continuous Gaussian beam normally incident to the PhC. To present the defocusing behavior within a short propagation distance, the beam waist and the peak amplitude of the incident wave were set as $w_0 = 7.5a$ (about 31.8 μm)

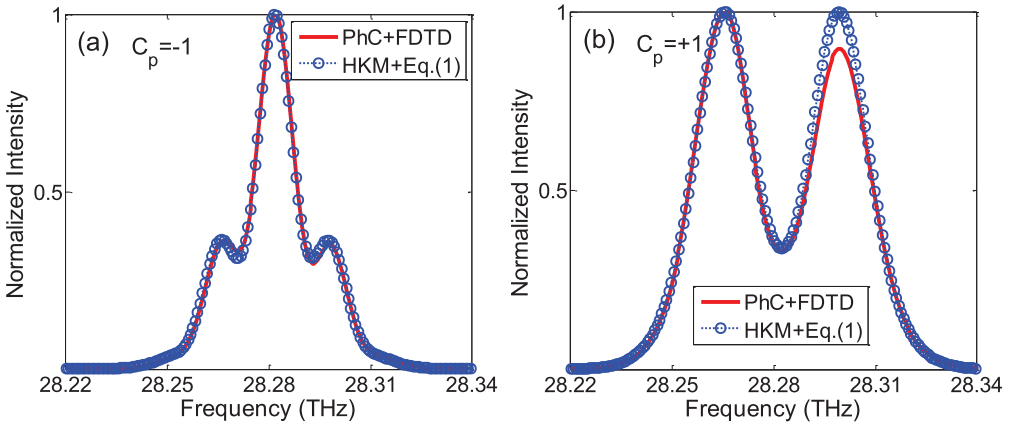

FIG. 3. (Color online) Normalized spectra of the pulses with opposite chirp parameter C_p after passing through a $701a$-thick nonlinear PhC (the solid lines) and a same thick HKM (the dotted lines marked with circles) of the same length: (a) $C_p = -1$, (b) $C_p = +1$.

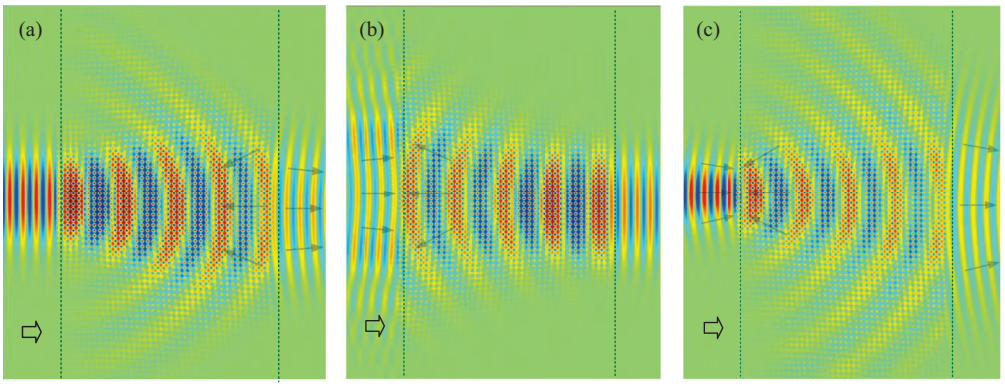

FIG. 5. (Color online) Self-defocusing in a nonlinear PhC with negative n_0 and positive n_2 for a high-power Gaussian incident beam with (a) planar, (b) diverging, and (c) converging wavefronts. Propagation is from left to right and the wave vectors in the PhC and free space are schematically denoted by the arrows.

and $E_0 = 9.0 \times 10^8$ V/m, respectively. As shown in Fig. 5(a), at the first interface between free space and the nonlinear PhC, the planar wavefront of the incident Gaussian beam of $\lambda = 10.6\,\mu$m became diverging just as if it were passing through a conventional concave lens. However, the diverging wavefront in the nonlinear PhC was changed into a converging one after it crossed the second interface. Therefore, merely in light of the input planar wavefront and the output converging wavefront, the nonlinear PhC effectively functions as a convex lens as if usual self-focusing occurs. The most striking difference between this self-defocusing and usual self-focusing is that the input beam becomes divergent in the nonlinear PhC, which spreads the peak power and protects the PhC from laser damage. More details can be achieved from the movie in the Supplemental Material [36], in which the divergent wavefront can be observed to be propagating opposite to the incident direction. This abnormal phenomenon can be explained by using the effective parameters of the nonlinear PhC as follows. The negative n_0 leads to the reversed propagation of the wavefront in the PhC, i.e., inverse diffraction. The opposite signs of n_0 and n_2 result in the central part of the beam propagating faster than the edge. Thus, the wavefront inside the nonlinear PhC has to be divergent so as to meet the requirement from the incident planar wavefront that the fast part and the slow part must arrive at the first interface simultaneously. Due to mirror effect of the negative refractive index, the defocusing wave in the PhC turns into a focusing one behind the second interface.

Besides the self-defocusing, more interestingly and importantly, the nonlinear PhC was also capable of controlling the nonlinear beam propagation by the incident wavefront. Since the linear refractive index n_0 is much less than unity, reverse diffraction in the PhC is amplified dramatically. As displayed in Fig. 5(b), an input Gaussian beam with a diverging wavefront was evidently focused in the same nonlinear PhC. At the first interface, the PhC turns the incident diverging wavefront in free space into a converging one because of its negative linear refractive index. Due to enhanced diffraction originating from the small n_0, the converging wavefront is supposed to be focused quickly, like self-focusing in conventional Kerr media. Nevertheless, in the nonlinear PhCs the central part of the wavefront propagates faster than the edge because of opposite signs of n_0 and n_2. Therefore, different from conventional self-focusing of convergent wavefront the focus in the nonlinear PhC is broadened and shifted toward the source [8,36]. For the same reason, the convergent wavefront of the input beam exaggerated the representation of the self-defocusing as shown in Fig. 5(c). Movies of Figs. 5(b) and 5(c) are also available in the Supplemental Material [36]. In addition, we have theoretically predicted similar phenomena in ideally conjectured negative-refractive-index materials [5,6,8]. However, that is still quite far from being realistic and practical, owing to the arbitrarily assumed parameters. The current work, for the first time, demonstrates the phenomenon in a realistic structure.

IV. CONCLUSION

To conclude, simultaneous control of self-defocusing and (or) self-focusing, which can be selectively enabled by the incident laser wavefront, has been demonstrated for the first time in the same nonlinear PhC made of Si pillars embedded in the liquid background of CS_2. In particular, the nonlinear refractive index coefficient of the PhC, responsible for the self-defocusing phenomenon, is retrieved by fitting the broadened spectrum resulting from the nonlinear propagation of chirped pulses inside the PhC to a theoretical model. The interplay between self-focusing and self-defocusing has been characterized. It is found that an incident beam with a diverging wavefront can be focused in the PhC quickly due to enhanced inverse diffraction caused by the linear n_0 of the PhC, while the focus is broadened and the peak power is reduced owing to the effect of self-defocusing governed by the nonlinear n_2 of the PhC. Such unusual phenomena, which are attributed to the negative n_0 and positive n_2, may give a distinct way to protect nanostructured devices from laser damage and provide a future method for manipulating laser propagation in PhCs. In addition, the presented approach and demonstrated control of focusing behavior in a nonlinear PhC can be readily extended to other periodic nanostructures such as metamaterials.

ACKNOWLEDGMENTS

The authors acknowledge Dr. Lei Zhang for preparing figures. This work was partially supported by the National

Natural Science Foundation of China (Grants No. 11076011, No. 61025024, and No. 61378002), Hunan Provincial Natural Science Foundation of China (Grant No. 12JJ7005), National High Technology Research and Development Program of China (863 Program, Grant No. 2012AA01A301-01), the Fundamental Research Funds for the Central Universities, and the visiting scholar program of China Scholarship Council.

[1] H. Kogelnik and T. Li, Appl. Opt. **5**, 1550 (1966).
[2] R. W. Boyd, S. G. Lukishova, and Y. R. Shen (eds.), *Self-focusing: Past and Present* (Springer, New York, 2009).
[3] R. W. Boyd, *Nonlinear Optics* (Academic Press, Boston, 2008).
[4] I. V. Shadrivov, A. A. Sukhorukov, and Y. S. Kivshar, Phys. Rev. E **69**, 016617 (2004).
[5] S. Wen, J. Wu, K. Tang, W. Su, X. Fu, and D. Fan, Proc. SPIE **5627**, 71 (2005).
[6] S. Wen, Y. Wang, W. Su, Y. Xiang, X. Fu, and D. Fan, Phys. Rev. E **73**, 036617 (2006).
[7] P. P. Banerjee and G. Nehmetallah, J. Opt. Soc. Am. B **24**, A69 (2007).
[8] Y. Hu, S. Wen, H. Zuo, K. You, and D. Fan, Opt. Express **16**, 4774 (2008).
[9] H. S. Eisenberg, Y. Silberberg, R. Morandotti, and J. S. Aitchison, Phys. Rev. Lett. **85**, 1863 (2000).
[10] R. Morandotti, H. S. Eisenberg, Y. Silberberg, M. Sorel, and J. S. Aitchison, Phys. Rev. Lett. **86**, 3296 (2001).
[11] D. R. Smith, W. J. Padilla, D. C. Vier, S. C. Nemat-Nasser, and S. Schultz, Phys. Rev. Lett. **84**, 4184 (2000).
[12] R. A. Shelby, D. R. Smith, and S. Schultz, Science **292**, 77 (2001).
[13] M. Notomi, Phys. Rev. B **62**, 10696 (2000).
[14] E. Cubukcu, K. Aydin, E. Ozbay, S. Foteinopoulou, and C. M. Soukoulis, Nature **423**, 604 (2003).
[15] P. V. Parimi, W. T. Lu, P. Vodo, and S. Sridhar, Nature **426**, 404 (2003).
[16] J. B. Pendry, A. J. Holden, D. J. Robbins, and W. J. Stewart, IEEE Trans. Microwave Theory Tech. **47**, 2075 (1999).
[17] T. Decoopman, G. Tayeb, S. Enoch, D. Maystre, and B. Gralak, Phys. Rev. Lett. **97**, 073905 (2006).
[18] V. Berger, Phys. Rev. Lett. **81**, 4136 (1998); N. G. R. Broderick, G. W. Ross, H. L. Offerhaus, D. J. Richardson, and D. C. Hanna, *ibid.* **84**, 4345 (2000); S. F. Mingaleev and Y. S. Kivshar, *ibid.* **86**, 5474 (2001).
[19] M. Soljacic, C. Luo, J. D. Joannopoulos, and S. Fan, Opt. Lett. **28**, 637 (2003).
[20] X. Yu, X. Jiang, and S. Fan, Appl. Phys. Lett. **90**, 161124 (2007).
[21] X. Jiang, C. Zhou, X. Yu, S. Fan, M. Soljacic, and J. D. Joannopoulos, Appl. Phys. Lett. **91**, 031105 (2007).
[22] G. A. Wurtz and A. V. Zayats, Laser Photon. Rev. **2**, 125 (2008); A. Arie and N. Voloch, *ibid.* **4**, 355 (2009).
[23] S. Larouche and D. R. Smith, Opt. Commun. **283**, 1621 (2010).
[24] A. Rose, S. Larouche, D. Huang, E. Poutrina, and D. R. Smith, Phys. Rev. E **82**, 036608 (2010).
[25] E. Poutrina, D. Huang, and D. R. Smith, New J. Phys. **12**, 093010 (2010).
[26] A. Rose, S. Larouche, E. Poutrina, and D. R. Smith, Phys. Rev. A **86**, 033816 (2012).
[27] Zhaxylyk A. Kudyshev, Martin C. Richardson, and Natalia M. Litchinitser, Nat. Commun. **4**, 2557 (2013).
[28] G. P. Agrawal, *Nonlinear Fiber Optics* (Academic Press, Singapore, 2013), Chap. 4.
[29] M. Oberthaler and R. A. Höpfel, Appl. Phys. Lett. **63**, 1017 (1993).
[30] B. R. Washburn, J. A. Buck, and S. E. Ralph, Opt. Lett. **25**, 445 (2000).
[31] M. T. Myaing, J. Urayama, A. Braun, and T. Norris, Opt. Express **7**, 210 (2000).
[32] R. L. Sutherland, *Handbook of Nonlinear Optics* (Marcel Dekker, New York, 2003), Chap. 8.
[33] Zhixiang Tang, Hao Zhang, Runwu Peng, Yunxia Ye, Lei Shen, Shuangchun Wen, and Dianyuan Fan, Phys. Rev. B **73**, 235103 (2006).
[34] Dong Jun Technology, EastFDTD v4.0 (Dongjun Information Technology Co., Shanghai, 2013).
[35] From the photonic band structure we obtained a group-velocity dispersion parameter $\beta_2 = 1.19 \times 10^{-3}$ ps$^2/\mu$m for the PhC at the operating wavelength $\lambda = 10.6$ μm. Then, the dispersion length L_D was found to be about $4.1 \times 10^5 \mu$m. Therefore, the propagating length L (about 3000 μm) is less than 1% of L_D.
[36] See Supplemental Material at http://link.aps.org/supplemental/10.1103/PhysRevA.91.063824 for the self-defocusing in the nonlinear PhC.
[37] Marin Soljačić and J. D. Joannapoulos, Nat. Mater. **3**, 211 (2004).
[38] Kuon Inoue, Hisaya Oda, Naoki Ikeda, and Kiyoshi Asakawa, Opt. Express **17**, 7206 (2009).
[39] Christos Argyropoulos, Pai-Yen Chen, Giuseppe D'Aguanno, Nader Engheta, and Andrea Alù, Phys. Rev. B **85**, 045129 (2012).